Structure-Function Relationship of the Chloroplastic Glutaredoxin S12 with an Atypical WCSYS Active Site*[S]

Jeremy Couturier[‡1], Cha San Koh[§1,2], Mirko Zaffagnini[¶1], Alison M. Winger[‡], Jose Manuel Gualberto[||], Catherine Corbier[**], Paulette Decottignies[‡‡], Jean-Pierre Jacquot[‡], Stéphane D. Lemaire[¶], Claude Didierjean[§3], and Nicolas Rouhier[‡4]

From the [‡]Unité Mixte de Recherches 1136 UHP-INRA Interaction Arbres-Microorganismes, IFR 110 GEEF, Nancy Université, Faculté des Sciences, 54506 Vandoeuvre Cedex, France, [§]LCM₃B, Equipe Biocristallographie, UMR 7036 CNRS-UHP Faculté des Sciences et Techniques, Nancy Université, BP 239, 54506 Vandoeuvre Cedex, France, [¶]Institut de Biotechnologie des Plantes, Université de Paris Sud, Bâtiment 630, 91405 Orsay Cedex, France, [||]Institut de Biologie Moléculaire des Plantes, CNRS, 67084 Strasbourg, France, [**]URAFPA, Equipe PB2P Faculté des Sciences et Techniques, Nancy Université, BP 239, 54506 Vandoeuvre Cedex, France, and [‡‡]Institut de Biochimie et Biophysique Moléculaire et Cellulaire, UMR 8619, CNRS/Université Paris-Sud 11, 91405 Orsay Cedex, France

Glutaredoxins (Grxs) are efficient catalysts for the reduction of mixed disulfides in glutathionylated proteins, using glutathione or thioredoxin reductases for their regeneration. Using GFP fusion, we have shown that poplar GrxS12, which possesses a monothiol [28]WCSYS[32] active site, is localized in chloroplasts. In the presence of reduced glutathione, the recombinant protein is able to reduce in vitro substrates, such as hydroxyethyldisulfide and dehydroascorbate, and to regenerate the glutathionylated glyceraldehyde-3-phosphate dehydrogenase. Although the protein possesses two conserved cysteines, it is functioning through a monothiol mechanism, the conserved C terminus cysteine (Cys[87]) being dispensable, since the C87S variant is fully active in all activity assays. Biochemical and crystallographic studies revealed that Cys[87] exhibits a certain reactivity, since its pK_a is around 5.6. Coupled with thiol titration, fluorescence, and mass spectrometry analyses, the resolution of poplar GrxS12 x-ray crystal structure shows that the only oxidation state is a glutathionylated derivative of the active site cysteine (Cys[29]) and that the enzyme does not form inter- or intramolecular disulfides. Contrary to some plant Grxs, GrxS12 does not incorporate an iron-sulfur cluster in its wild-type form, but when the active site is mutated into YCSYS, it binds a [2Fe-2S] cluster, indicating that the single Trp residue prevents this incorporation.

Glutaredoxins (Grxs)[5] are GSH- or thioredoxin reductase-dependent oxidoreductases involved in the maintenance of cellular redox homeostasis. When Grxs are recycled by GSH, the GSSG formed is in turn reduced by NADPH and glutathione reductase (GR), forming the GSH/Grx reducing system. The first Grxs characterized usually contained the active site motif Cys-Pro-Tyr-Cys, the second active site cysteine being generally not essential for Grx activity (1, 2). It has been shown, however, to be required for a few reactions, such as the reduction of some low molecular weight disulfides or of disulfide bonds in E. coli ribonucleotide reductase and phosphoadenylyl-sulfate reductase (1, 3, 4). In most cases, Grxs rather reduce specifically protein-glutathione adducts via two distinct mechanisms. The monothiol mechanism requires only the more N terminus active site cysteine together with two glutathione molecules, and the dithiol mechanism requires either the two active site cysteines or the N terminus active site cysteine and a conserved extra active site C terminus cysteine. Both types of disulfides formed on Grx are reduced in vitro by GSH or thioredoxin reductases (1, 4–7). In comparison, thioredoxins (Trxs) efficiently reduce protein disulfides but have low or no activity with mixed disulfides (7, 8). Sharing high structural and functional homologies with Trx, Grxs display a common Trx fold (9). The CXXC motif in Trx and Grx is located in a partially exposed surface loop downstream of a β-strand and at the N terminus of an α-helix (9). Interestingly, some Trxs and Grxs only contain the N terminus cysteine of the CXXC motif, the second cysteine being very often replaced by a serine. In plants, this variation of active site sequence exists in approximately

half of the 30 Grxs existing (10). Grxs were initially categorized, based on the active site sequence, into two groups, a dithiol (CPY/FC motif) and a monothiol (CGFS motif) subgroup (11). Nevertheless, the increasing number of Grxs with primary structures that deviate from these standard motifs has led to the proposal of a more appropriate and thorough classification of plant Grxs (10, 12, 13). Three subclasses have been defined based on their active site structures. Subclass I includes proteins with CXX(C/S) active sites other than CGFS, subclass II contains exclusively Grxs with a CGFS motif, and subclass III, which is specific to land plants, corresponds to Grxs with a peculiar CCXX active site.

Many structures of dithiol Grxs from human (Protein Data Bank codes 1JHB, 2CQ9, 2FLS, 2HT9, 1B4Q), pig (Protein Data Bank code 1KTE), mouse (PDB codes 1T1V, 1WJK), plant (Protein Data Bank codes 1Z7P, 1Z7R, 2E7P), yeast (Protein Data Bank code 2JAC), bacteria (Protein Data Bank codes 1EGR, 1EGO, 1FOV, 1GRX, 1G7O, 1H75, 2AYT, 1J08, 1R7H, 2YWM), virus (Protein Data Bank codes 2HZE, 2HZF), or T4 bacteriophage (Protein Data Bank codes 1DE1, 1DE2, 1AAZ, 1ABA, 1QFN, 3GRX) have been solved by NMR spectroscopy or x-ray crystallography both in the oxidized and reduced forms. Some of these Grx structures contain either a low molecular weight substrate or an interacting peptide partner. Only one NMR structure (*Escherichia coli* Grx4, PDB code 1YKA) of monothiol Grx is available despite the abundance of genes reported.

In this study, we have investigated the structure-function relationship of a monothiol Grx isoform (GrxS12) found in *Populus tremula × tremuloides*, which possesses an unusual [28]WCSYS[32] active site sequence, unique to plants. Phylogenetic analyses indicate that GrxS12 belongs to Grx subclass I, along with classical dithiol Grxs. In addition to the active site cysteine, there is an additional C terminus cysteine in position 87, which is present in many dithiol or monothiol Grxs. Its role remains obscure, although it has been demonstrated that it can serve as a resolving cysteine of the glutathionylated catalytic cysteine in a few organisms (5–7). Biochemical and enzymatic studies of mutated proteins together with the resolution of liganded GrxS12 structures allowed us (i) to identify the GSH binding site of this enzyme, (ii) to investigate the role of the C terminus cysteine in the catalytic mechanism of GrxS12, and (iii) to understand why an iron-sulfur cluster is not present in GrxS12 despite its apparently favorable CSYS motif.

EXPERIMENTAL PROCEDURES

Materials—NAP-5 columns were purchased from GE Healthcare. Hydroxyethyldisulfide (HED) and 5,5′-dithiobis-2-nitrobenzoic acid were from Aldrich and Pierce, respectively. All other reagents were from Sigma.

Cloning and Construction of GrxS12 Mutants by Site-directed Mutagenesis—The open reading frame sequence encoding poplar GrxS12 was amplified from a *P. tremula × tremuloides* leaf cDNA library using GrxS12 forward and reverse primers (supplemental Table 1) and cloned into the NcoI and BamHI restriction sites (underlined in the primers) of pET3d (Novagen). The sequence amplified encodes a protein deprived of the first 74 amino acids corresponding to the putative targeting

sequence and in which a methionine and an alanine have been added during cloning. The protein starts thus with the N terminus sequence [1]MASFGSRL[8] and ends with [98]AKKSQG[113] at the C terminus (see supplemental Fig. 1). Using two complementary mutagenic primers, the two cysteines of GrxS12 were individually substituted into serines, the Trp in position 28 was mutated into Tyr, and the active site was also entirely modified from WCSYS into YCGYC. The primers are listed in supplemental Table 1. The mutated proteins are called GrxS12 W28Y, C29S, and C87S and GrxS12 YCGYC.

Expression and Purification of the Recombinant Proteins—For protein production, the *E. coli* BL21(DE3) strain, containing the pSBET plasmid, was co-transformed with the different recombinant plasmids (14). Cultures were successively amplified up to 2.4 l in LB medium supplemented with ampicillin and kanamycin at 37 °C. Protein expression was induced at exponential phase by adding 100 μM isopropyl β-D-thiogalactopyranoside for 4 h at 37 °C.

The cultures were then centrifuged for 15 min at $4400 \times g$. The pellets were resuspended in 30 ml of TE NaCl (30 mM Tris-HCl, pH 8.0, 1 mM EDTA, 200 mM NaCl) buffer, and the suspension was conserved at −20 °C.

Cell lysis was performed by sonication (3×1 min with intervals of 1 min), and the soluble and insoluble fractions were separated by centrifugation for 30 min at $27,000 \times g$. The soluble part was then fractionated with ammonium sulfate in two steps, and the protein fraction precipitating between 40 and 80% of the saturation contained the recombinant protein, as estimated by 15% SDS-PAGE. The protein was purified by size exclusion chromatography after loading on an ACA44 (5×75-cm) column equilibrated in TE NaCl buffer. The fractions containing the protein were pooled, dialyzed by ultrafiltration to remove NaCl, and loaded onto a DEAE-cellulose column (Sigma) in TE (30 mM Tris-HCl, pH 8.0, 1 mM EDTA) buffer. All of the proteins (GrxS12 WT, W28Y, C29S, C87S, and YCGYC) passed through the DEAE column and were subsequently loaded onto a carboxymethylcellulose column (Sigma) in TE buffer. The proteins were eluted using a 0–0.4 M NaCl gradient. Finally, the fractions of interest were pooled, dialyzed, concentrated by ultrafiltration under nitrogen pressure (YM10 membrane; Amicon), and stored in TE buffer at −20 °C. Purity was checked by SDS-PAGE. Protein concentrations were determined spectrophotometrically using a molar extinction coefficient at 280 nm of 9970 M^{-1} cm^{-1} for the GrxS12 WT, C29S, and C87S and 5960 M^{-1} cm^{-1} for GrxS12 W28Y and GrxS12 YCGYC.

In Vivo Subcellular Localization—A fragment of 285 nucleotides coding for the 95 first amino acids of GrxS12 was cloned in the 5′-part of the GFP coding sequence under the control of a double ^{35}S promoter into the plasmid pCK-GFP3 using GrxS12 pCK forward and reverse primers (supplemental Table 1). *Nicotiana benthamiana* epidermal leaf cells were transfected by bombardment of the abaxial side of young leaves with tungsten particles coated with plasmid DNA. Images were obtained 18 h later with a Zeiss LSM510 confocal microscope. Stomata cells were preferentially imaged, because of their small size and because typically only one of the two guard cells is transfected and expresses the GFP construction, whereas the untransfected

cell serves the role of internal negative control. Chloroplasts were visualized by the natural fluorescence of chlorophyll.

Reduction and Oxidation of Wild-type and Mutated GrxS12— The proteins (50–100 μM) were reduced by 10 mM DTT for 1 h at 25 °C, followed by desalting on NAP-5 column pre-equilibrated with 30 mM Tris-HCl, pH 7.9. Oxidized Grxs were prepared by incubation of prereduced with 10 mM oxidized DTT or 1–5 mM GSSG for 1–2 h at 25 °C. GSSG-oxidized GrxS12 (WT or mutants) were desalted as above and treated by 10 mM reduced DTT or by 2 mM GSH in the presence of 6 μg/ml yeast glutathione reductase and 0.5 mM NADPH.

*Mass Spectrometry Analysis—*Reduced and oxidized GrxS12 WT and C87S and trypsin-cleaved proteins were analyzed by MALDI-TOF MS as described in Ref. 15.

Fluorescence Properties of Wild-type and Mutated GrxS12— The fluorescence characteristics of GrxS12 and GrxS12 C87S in the reduced and oxidized forms were recorded with a spectrofluorometer (Cary Eclipse; VARIAN) in TE buffer with a 10 μM concentration of each protein.

*Determination of Free Thiol Groups—*The number of free thiol groups in untreated, reduced, or oxidized proteins was determined spectrophotometrically with 5,5'-dithiobis-2-nitrobenzoic acid, as described in Ref. 7.

*pK_a Determination of GrxS12 Sulfhydryls with (2-pyridyl)dithiobimane (PDT-bimane)—*The reaction of PDT-bimane with cysteine forms pyridine-2-thione, which has a maximum absorption wavelength of 343 nm (16). The stock solution of PDT-bimane was made in DMSO, and the concentration was determined using the absorbance extinction coefficient at 380 nm, $\epsilon_{380} = 5000$ M^{-1} cm^{-1} in ethanol. Reactions were started by the addition of PDT-bimane to a final concentration of 25 μM into a cuvette containing 10 μM reduced proteins in 500 μl of sodium citrate or phosphate buffer ranging from pH 3.0 to 8.0 and rapidly mixed, and the absorbance at 343 nm was recorded over 120 min with a Varian Cary 50 spectrophotometer. Absorbance data were fitted directly to the Michaelis-Menten equation with the GraphPad Prism 5 program and the $t_{1/2}$ (the time to reach half-maximal reactivity as monitored by half-maximal release of pyridyl-2-thione) at each pH was determined. Those values were plotted against pH using sigmoidal curve fit and GraphPad Prism 5 (GraphPad software).

*Activity Measurements—*The activity measurements of WT or mutant GrxS12 in the HED assay or for reduction of DHA or glutathionylated GAPDH were performed as described in Zaffagnini *et al.* (7).

*Crystallization, Data Collection, Structure Determination, and Crystallographic Refinement—*The complex of poplar GrxS12 with glutathione (GrxS12·GSH) was directly obtained using the purified recombinant protein. The complex of GrxS12 with both GSH and β-mercaptoethanol (βMSH) (GrxS12·GSH·βMSH) was prepared after purification steps by the addition of 2 mM GSH and 10 mM HED to the purified recombinant protein for 2 h at room temperature prior to extensive dialyses against TE buffer to remove unbound GSH, HED, or βMSH.

Crystals were grown at 20 °C by the microbatch under oil (paraffin) method. Optimal crystallization conditions were screened based on the sparse matrix crystallization approach.

The protein at an initial concentration of 10–15 mg ml^{-1} in TE buffer was mixed with similar precipitant solutions (for each protein) in a 1:1 ratio. The GrxS12·GSH crystals were obtained by using 0.1 M Na-HEPES (pH 7.5) and 20% polyethylene glycol 8000 solution (JBS 5-B4), whereas GrxS12·GSH·βMSH crystallized in 0.1 M Na-HEPES (pH 7.5) and 25% polyethylene glycol 1000 solution (JBS 1-C3). Grx crystals grew rapidly within 2 days.

X-ray diffraction data were collected from single crystals flash-cooled in a nitrogen stream at 100 K. Data of both complexes, GrxS12·GSH and GrxS12·GSH·βMSH, were collected on a MAR165 CCD detector at beamlines X11 and X13 (DESY/EMBL, Hamburg, Germany), respectively. All crystallographic data were indexed, processed, and scaled with *HKL*-2000 (17). Data collection and refinement statistics are summarized in Table 1. The crystal structure of GrxS12·GSH was determined by molecular replacement with MOLREP (18, 19), using human Grx2 (Protein Data Bank code 2FLS) as a model (20). The resulting solution coordinates were used for automatic model building using the program ARP/wARP (21). After 75 cycles of autobuilding, 99% of the model (786 atoms were refined) was built automatically. Hence, the initial model of GrxS12·GSH comprises 100 residues with a connectivity index of 0.96 and R factor of 19.5%. This structure was then refined using REFMAC version 5.4 (18, 22) interspersed with manual inspection using COOT (23). A GSH molecule was added almost toward the end of the refinement of the GrxS12·GSH model. The coordinates of GrxS12·GSH were then used to solve the structure of GrxS12·GSH·βMSH, also by molecular replacement. The structure refinement of the latter was done as for the template. Positions of water molecules were identified with ARP/wARP and were checked manually. The validation of both crystal structures was performed with PROCHECK (24). All figures were prepared with PyMOL (25). Structure superimpositions were performed using the LSQMAN program from the DEJAVU package (26) or Lsqkab (superpose) program of the CCP4 package.

RESULTS

*Subcellular Localization of GrxS12—*The genome analysis of *Populus trichocarpa* suggests that at least four Grxs should be located in the chloroplast. Two Grxs of subgroup II, possessing a CGFS active site and called GrxS14 and GrxS16, have been experimentally shown to be located in plastids and would be involved in iron-sulfur biogenesis, since they incorporate an iron-sulfur cluster that can be transferred very quickly to apoferredoxin (27). The GrxS12 from *P. tremula* × *tremuloides* is a protein of 185 amino acids with a predicted chloroplastic N terminus-targeting sequence. In order to experimentally confirm its localization, the sequence coding the first 95 amino acids, including thus the putative targeting sequence and the first α-helix and β-strand, was fused to the GFP coding sequence and used to bombard tobacco leaf cells. As shown in Fig. 1, the fluorescence associated with this construction, transfected into one of the two guard cells of a stomate, strictly colocalizes with the autofluorescence of chlorophyll, indicating that the protein is indeed chloroplastic.

TABLE 1

Data collection and refinement statistics for GrxS12·GSH and GrxS12·GSH·βMSH crystals

Data set	GrxS12·GSH	GrxS12·GSH·βMSH
Data collection and processing statistics		
Data collection site	X11 DESY/EMBL-Hamburg	X13 DESY/EMBL-Hamburg
Wavelength (Å)	0.8150	0.8063
Space group	P2$_1$2$_1$2$_1$	P2$_1$2$_1$2$_1$
Unit cell dimensions (Å) (*a, b, c*)	39.03, 47.27, 55.62	38.83, 46.82, 55.36
Asymmetric unit	1 subunit	1 subunit
Resolution range (Å)[a]	50.00–1.70 (1.73–1.70)	50.00–1.80 (1.86–1.80)
Redundancy [a]	4.49 (4.16)	6.69 (6.85)
Completeness (%)[a]	99.7 (95.0)	99.6 (100.0)
$I/\sigma I$ [a]	13.37 (2.26)	23.26 (16.95)
R_{merge} [a,b]	0.045 (0.239)	0.048 (0.107)
Refinement statistics		
Resolution range (Å)	36.0–1.70	30.0–1.80
Reflections used	11,234	9301
R_{cryst} [c] (R_{free})[d]	19.28 (23.95)	16.78 (21.45)
Protein/waters/GSH/HED	106 residues/186/1/0	106 residues/186/1/0
Mean *B* factor (Å^2)		
Main chain	16.53	12.04
Side chain	23.33	14.79
Water	32.57	27.88
Ligand	15.31	17.00
All	20.52	16.24
r.m.s. deviation from ideal geometry		
Bond lengths (Å)	0.012	0.011
Bond angles (degrees)	1.4	1.4
Dihedral angles (degrees)	23.5	23.7
Improper angles (degrees)	1.61	1.75
Ramachandran plot		
Residues in most favored regions (%)	96.7	95.6
Residues in additionally allowed regions (%)	3.3	4.4
Residues in generously allowed regions (%)	0.0	0.0

[a] $R_{cryst} = \Sigma|F_o - F_c|/\Sigma F_o$, where F_o and F_c are the observed and calculated structure factor amplitudes, respectively.
[b] The R_{free} value was calculated from 5% of all data that were not used in the refinement.
[c] $R_{cryst} = \Sigma|F_o - F_c|/\Sigma F_o$, where F_o and F_c are the observed and calculated structure factor amplitudes, respectively.
[d] R_{free} is as for R_{cryst} but calculated for a test set comprising reflections not used in the refinement (5%).
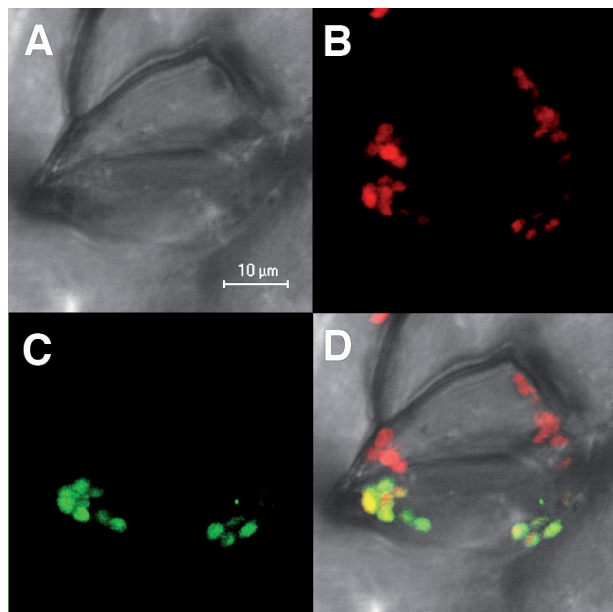

FIGURE 1. **GFP localization of GrxS12 in plant guard cells.** *A*, cells under visible light; *B*, autofluorescence of chlorophyll (*red*); *C*, fluorescence of the GFP construction; *D*, merged images.

Determination of GrxS12 Redox States by Fluorescence, Thiol Titration, and Mass Spectrometry—The recombinant protein produced in *E. coli* is a protein containing 113 residues devoid of the first 74 N terminus residues (which represent the transit peptide) and in which a methionine and an alanine have been added in the new N terminus end. The predicted molecular

TABLE 2

Number of free thiols in WT and C87S GrxS12 under various redox conditions

The untreated column is indicative of the protein thiol content measured after purification. GrxS12 was reduced by DTT$_{red}$ and subsequently oxidized by DTT$_{ox}$ or GSSG. After each treatment (DTT$_{red}$, DTT$_{ox}$, and GSSG), samples were desalted. The thiol content per protein was quantified by 5,5'-dithiobis(nitrobenzoic acid). Data are represented as mean ± S.D. (*n* = 4). ND, not determined.

	Untreated	DTT$_{red}$ treatment	DTT$_{ox}$ treatment	GSSG treatment
GrxS12	0.821 ± 0.078	1.98 ± 0.269	1.9 ± 0.1	0.808 ± 0.029
GrxS12 C87S	0.115 ± 0.017	1.056 ± 0.125	ND	0.132 ± 0.053

mass and pI are 12,360 Da and 8.56, respectively. A MALDI-TOF analysis of the purified GrxS12 WT revealed two protein peaks with molecular masses of 12,229.1 and 12,535.7 Da (data not shown). The first one is consistent with a protein where the methionine is cleaved, which is not surprising, since the second residue is an alanine, and the second peak is consistent with a glutathionylated protein also deprived of the methionine (306.6 Da mass increase compared with peak 1). There are two conserved cysteine residues in GrxS12, the active site cysteine in position 29 and a C terminus cysteine in position 87. In some CGFS Grxs, the latter cysteine can form an intramolecular disulfide with the catalytic cysteine (5–7). In order to check the possibility that Cys[87] acts as a recycling cysteine in GrxS12, we measured the number of free thiol groups under reducing and oxidizing conditions in GrxS12 WT and C87S (Table 2). After purification and in the absence of any reducing or oxidizing treatment (native form), GrxS12 WT possesses about one free thiol group, whereas there is no free thiol in GrxS12 C87S. A
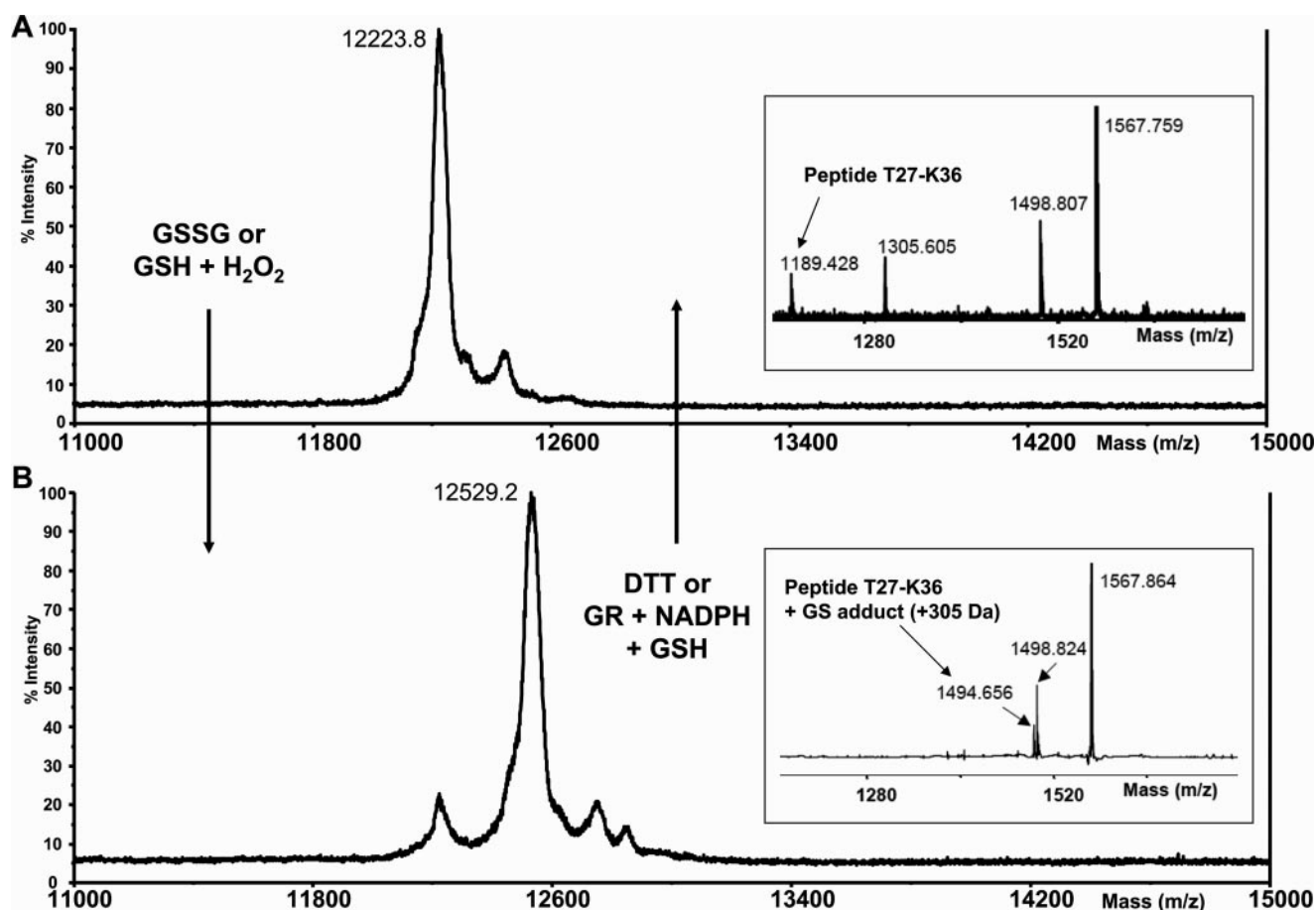
FIGURE 2. **MALDI-TOF mass spectrometry analysis of reduced or glutathionylated GrxS12.** MALDI-TOF spectra of whole protein or after tryptic digestion (*insets*) were determined for reduced GrxS12 before (*A*) or after (*B*) glutathionylation treatments (5 mM GSSG or 0.1 mM H_2O_2 plus 0.5 mM GSH for 1 h). The shifted peptide (Thr[27]–Lys[36]) is indicated. The 305 Da shift after glutathionylation treatment could be reversed by treatments with 10 mM DTT or with 2 mM GSH in the presence of 6 μg/ml yeast glutathione reductase and 0.5 mM NADPH. Similar results were obtained with the WT and C87S GrxS12.

reduction by DTT_{red} led to the expected number of free thiols, two for the WT and one for the C87S mutant. After a prereduction step of WT GrxS12, a subsequent oxidation by DTT_{ox} over a long period (2 h) did not change these values, indicating that no intra- or intermolecular disulfide bridges can be formed. Such disulfides have not been observed on nonreducing SDS-polyacrylamide gels either (data not shown). On the contrary, subsequent oxidation using 1 mM GSSG gave the same values as those found originally in the untreated proteins, one free thiol group for GrxS12 WT but no free thiol in GrxS12 C87S. Together, these results suggest the presence of a glutathione adduct on the catalytic cysteine (Cys[29]), whereas the second cysteine (Cys[87]) is not modified. In order to confirm these results, we analyzed by MALDI-TOF mass spectrometry prereduced GrxS12 before or after glutathionylation treatments in the presence of GSSG or GSH and H_2O_2 (Fig. 2). After treatment, the mass of the protein increased by ~305 Da, a feature consistent with the formation of one glutathione adduct. This increase was reversed by treatment with either DTT_{red} or GSH/GR/NADPH. A similar behavior was observed for WT or C87S GrxS12, indicating that Cys[29] is indeed the residue modified by glutathionylation. This was further confirmed by tryptic digestion and peptide mass fingerprinting of reduced or glutathionylated GrxS12. Indeed, the peptide (Thr[27]–Lys[36]) containing

Cys[29] is shifted by 305 Da in the glutathionylated protein. All of these results indicate that Cys[29] is undergoing glutathionylation, whereas Cys[87] is not glutathionylated in any of the conditions tested.

GrxS12 contains a single tryptophan adjacent to the active site. Given that proximity, we have investigated whether the intrinsic fluorescence of GrxS12 could change under reducing (GSH or DTT_{red}) or oxidizing (GSSG or DTT_{ox}) conditions. Reduced GrxS12 displays an emission spectrum with a maximum at 350 nm characteristic of a fluorescence signal strongly dominated by Trp (Fig. 3). Adding 1 mM GSSG to reduced GrxS12 immediately led to the disappearance of the fluorescence signal. The addition of DTT_{red} restored the initial spectrum (data not shown). Similar results were obtained with GrxS12 C87S, indicating that the tryptophan environment strongly changed after glutathionylation of the first active site cysteine. In accordance with thiol titrations, the addition of DTT_{ox} did not change the GrxS12 fluorescence spectrum.

Dehydroascorbate Reductase Activity, HED Assay, and Reduction of Glutathionylated A4-GAPDH—GrxS12 was found to be active in the two classical GRX assays: the reduction of DHA and HED assays. The activity of GrxS12 in these two assays displayed a linear relationship with increasing protein concentrations in the 0–0.75 μM and 0–100 nM
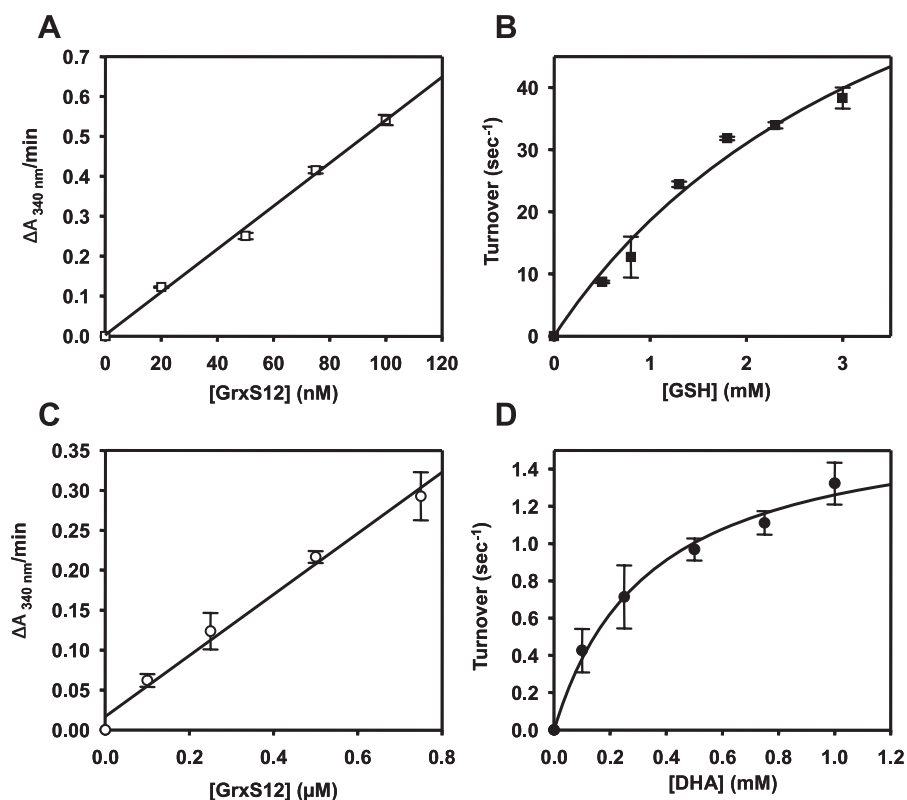
ranges, respectively (Fig. 4, *A* and *C*). The kinetic analyses revealed catalytic efficiency values (k_{cat}/K_m) comparable to those reported for other GrxS to subclass I. (Fig. 4, *B* and *D*, and Table 3).

We have recently demonstrated that A_4-GAPDH activity is reversibly inhibited by glutathionylation (28). This chloroplastic protein, which participates in the Calvin cycle, can be used as a more physiological substrate to test deglutathionylation activ-
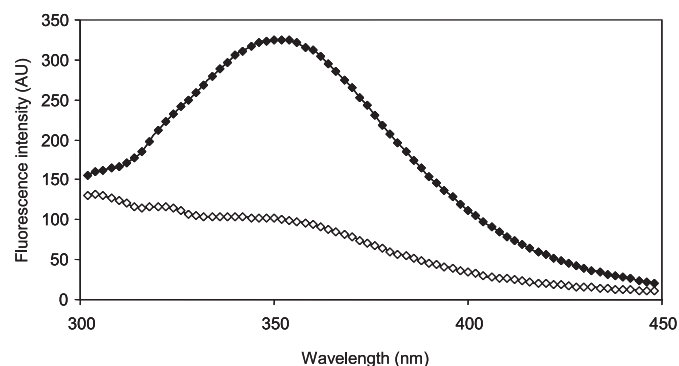
FIGURE 3. **Fluorescence spectra of poplar GrxS12 under different redox states.** Emission spectra of reduced (◆) and oxidized (◇) GrxS12 (excitation at 290 nm) were recorded with 10 μM protein at 25 °C in TE, pH 8.0, buffer. The reduced GrxS12 was obtained by a pretreatment of the protein with 10 mM DTT. GrxS12 was oxidized using 1 mM GSSG after DTT prereduction. In each case, residual compounds were removed by gel filtration.

ity. In order to obtain glutathionylated A_4-GAPDH, the protein was incubated in the presence of 0.1 mM H_2O_2 plus 0.5 mM GSH. Subsequently, the ability of WT and monocysteinic variants of GrxS12 to recover GAPDH activity was determined (Fig. 5A). Using a GSH/GR/NADPH reduction system, WT and C87S GrxS12 allowed recovery of ~50% of GAPDH initial activity, whereas no reactivation was observed with the C29S mutant. The recovery of GAPDH activity obtained in the presence of GrxS12 did not reach the levels obtained in the presence of DTT (~90%). This can be explained by the fact that H_2O_2 plus GSH leads to glutathionylation but also to primary oxidation of the catalytic cysteine of GAPDH to sulfenic acid, the latter being more efficiently reduced by 20 mM DTT than by the Grx system (28). The kinetic parameters of GAPDH deglutathionylation by GrxS12 were determined (Fig. 5B). With an $S_{0.5}$ of 3.7 ± 0.7 μM and a $t_{0.5}$ around 2–3 min, GrxS12 exhibits a catalytic efficiency comparable with other Grxs from *Chlamydomonas reinhardtii* (7).

In all of these assays (DHA, HED, and GAPDH assays), GrxS12 C87S appeared as efficient as the WT protein. These results indicate that in these assays, GrxS12 activity relies on a monothiol mechanism involving only Cys[29]. Nevertheless, at higher concentrations (10 times more than the WT), the GrxS12 C29S mutant exhibited an activity slightly above the background activity in the HED assay (data not shown). In order to know whether Cys[87] is reactive in this mutant, the pK_a of both cysteines was measured using the thiol-cleavable fluorophore PDT-bimane (Fig. 6). From the plot of the $t_{1/2}$ of half-maximal release of pyridyl-2-thiolate against pH, the pK_a of Cys[29] is ~2.8, a value in the range of those determined for mammalian Grxs, and the pK_a of Cys[87] is ~5.6 (29). Thus, the C terminus Cys[87] is in the thiolate form at the pH of the activity assays and thus at physiological pH. In addition, since this cysteine is surface exposed (see below), it should thus be able to perform a nucleophilic attack on an accessible disulfide.

Structure of GrxS12 and Quality of the Models—The two liganded forms of the enzyme (GrxS12·GSH and GrxS12·GSH·βMSH) crystallized in the orthorhombic system with similar unit cell parameters and with a monomer in the asymmetric unit. Both structures have been determined at 1.70 and 1.80 Å resolutions for GrxS12·GSH and GrxS12·GSH·βMSH, respectively.

Overall structures are well defined in the $2F_o - F_c$ electron density map except for a few N terminus residues and some lateral chains

FIGURE 4. **HED and DHA reductase activity of poplar GrxS12.** *A* and *C*, linear dependence of HED (*A*) and DHA reductase (*C*) activity on GrxS12 concentration expressed as ΔA_{340}/min. The data are represented as mean ± S.D. *B* and *D*, variations of the apparent turnover number during an HED assay catalyzed by 50 nM GrxS12 in the presence of GSH concentrations ranging from 0.5 to 3 mM (*B*) and during DHA reduction catalyzed by 0.25 μM GrxS12 in the presence of varying DHA concentrations ranging from 0.1 to 1 mM (*D*). Turnover represents mol of NADPH oxidized/s by 1 mol of GrxS12. Activity was calculated after subtracting the spontaneous reduction rate observed in the absence of GrxS12. Three separate experiments were performed, and the data are represented as mean ± S.D. The best fit was obtained using the Michaelis-Menten equation.

TABLE 3

Kinetic parameters of GrxS12 in HED and DHA activity assays

The apparent K_m value for GSH in the HED assay was determined using a GSH concentration range of 0.5–3.0 mM in the presence of 0.7 mM HED. The apparent K_m value for DHA was determined using a concentration range of 0.1–1 mM in the presence of 2 mM GSH. The apparent K_m and apparent turnover values (k_{cat}) were calculated by nonlinear regression using the Michaelis-Menten equation. Data are represented as mean ± S.D. ($n = 3$).

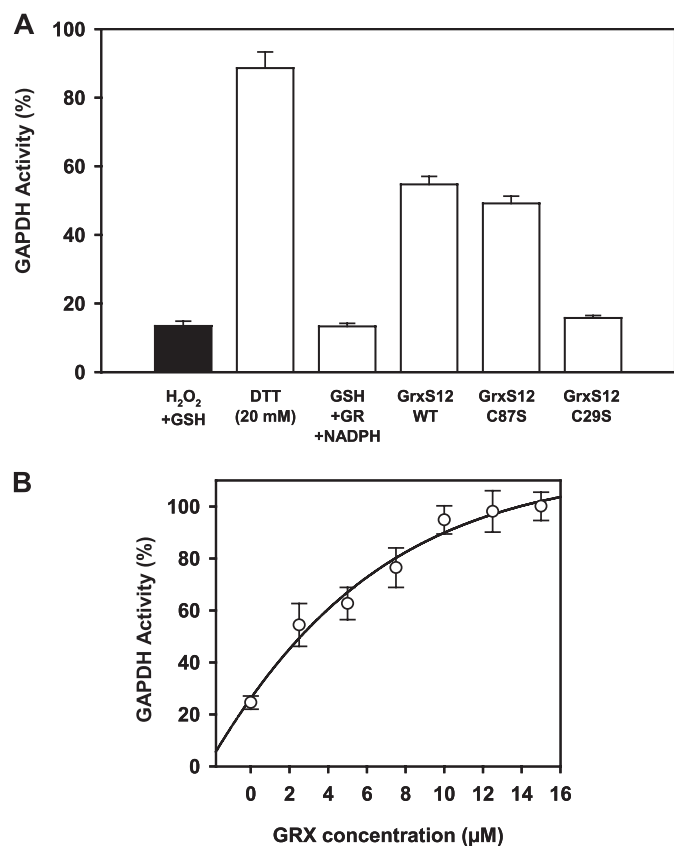|	K_m	k_{cat}	k_{cat}/K_m
	mM	s^{-1}	$M^{-1} s^{-1}$
DHA	0.38 ± 0.19	1.73 ± 0.19	4.6×10^3
GSH	3.99 ± 0.48	92.78 ± 5.32	2.33×10^4

FIGURE 5. **Reactivation of glutathionylated A$_4$-GAPDH.** A$_4$-GAPDH was inactivated by incubation with 0.1 mM H$_2$O$_2$ in the presence of 0.5 mM GSH for 15 min at 25 °C and subsequently treated with 35 μM 1,3-bisphosphoglycerate. *A*, the reactivation assays were performed under the following conditions: (i) 20 mM DTT, (ii) 2 mM GSH in the presence of 6 μg/ml yeast glutathione reductase and 0.2 mM NADPH alone or (iii) in the presence of 10 μM GrxS12 WT, C29S, or C87S. The NADPH-dependent activity was determined before (*black bar*) and after the different reactivation treatments (*white bars*). *B*, reactivation of glutathionylated A$_4$-GAPDH with 2 mM GSH, 6 μg/ml yeast glutathione reductase, 0.2 mM NADPH in the presence of varying concentrations of GrxS12 ranging from 2.5 to 15 μM. Activities are represented as a percentage of the initial activity measured before the inactivation treatment. The data are shown as mean ± S.D.

that are solvent-exposed. The final models contain 106 amino acid residues, corresponding to residues from Gly[5] to Lys[110]. A GSH molecule could be easily located in both models, at the active site covalently bound to Cys[29]. In the GrxS12·GSH·βMSH structure, a βMSH molecule can also be modeled covalently bound to the extra cysteine (Cys[87]) at the C terminus of the glutathionylated enzyme.

Superimposition between both liganded structures gives the r.m.s. deviation value of 0.162 Å (based on alignments of 106 Cα

positions). These low r.m.s. deviation values suggest that binding of a βMSH molecule did not induce significant variations within these structures. Therefore, unless indicated otherwise, our discussion by default will be based on the structure of GrxS12·GSH because of its better structure resolution.

The overall subunit structure of GrxS12 shows no significant differences from other known Grxs. They all display a Trx fold with/without some secondary structure extensions. Poplar GrxS12 has an N terminus α helix (namely α_1' in this study; see Fig. 7 and supplemental Table 2) in addition to the Trx fold. This additional secondary structure is also present in most Grxs, including human Grx2 (Protein Data Bank code 2FLS), poplar GrxC1 (PDB code 2E7P), yeast Grx1P (Protein Data Bank code 2JAC), and *E. coli* monothiol Grx4 (Protein Data Bank code 1YKA) but not in T4 bacteriophage Grx (Protein Data Bank code 1ABA) nor in *E. coli* Grx1 (Protein Data Bank code 1GRX) and Grx3 (Protein Data Bank code 3GRX). A structural evaluation of the conserved residues between GrxS12 and its orthologs reveals that residues that constitute β1, β3, and β4 are highly conserved (supplemental Fig. 1).

Active Site—The active site of the enzyme is hosting a GSH molecule that is covalently bound to Cys[29] and noncovalently stabilized by three neighboring loops between β1-α1', α2-β3, and β4-α3 (composed of [28]WCSY[31], [73]TVP[75], and [86]GCT[88]; referred to as the GSH binding site in this paper; see Fig. 7). The boundary loops that support the glutathione binding are in their usual conformations as observed for other Grxs. We describe here, for the first time, the crystal structure of glutaredoxin of subclass I with the active site motif [29]CSYS[32] (in comparison with the classical CPY/FC motif for dithiol Grxs and CGFS for monothiol Grxs). Despite the replacement of a Pro present in the Grx counterparts possessing a CPY/FC motif (with ϕ and ψ values of approximately $-53°$ and $-40°$, respectively) by a Ser (Ser[30]) in the CSYS motif of GrxS12 (with ϕ and ψ values of $-60.47°$ and $-40.18°$, respectively), they adopt the same backbone conformation. GrxS12 also possesses a second Ser residue at the active site in which the Ser[32] replaces the common C terminus active site Cys of dithiol Grxs. Ser[32] is hydrogen-bonded (2.50 Å) to another nearby conserved serine residue (Ser[25]). The latter residue could play an important role in stabilizing the active site, since it is conserved in all Grxs with a CXXS active site motif.

It is interesting to note that residue Trp[28] at the active site of GrxS12 (WCSYS) is well conserved in all plant GrxS12 orthologs and also in *Arabidopsis* GrxC5 (WCSYC) orthologs but not in other known Grxs. In the poplar GrxS12 structure, the position of Trp[28] (χ1 value = $+52.71°$) is similar to most other classical thioredoxins (χ1 values between $+40°$ and $+55°$), and its side chain covers an important part of the active site surface in the glutathionylated form, but fluorescence experiments indicate that it would adopt another conformation in the reduced form. The χ1 value of Trp[28] is similar to those described for other residues at the corresponding position in other Grxs ($+57.57°$ for Tyr[29] of poplar GrxC1 and $+67.64°$ for Ser[36] of human Grx2).

In GrxS12, the GSH binding site constitutes a groove, mainly populated by polar residues, along which the backbone atoms of GSH are positioned (this is where GrxS12 accommodates the
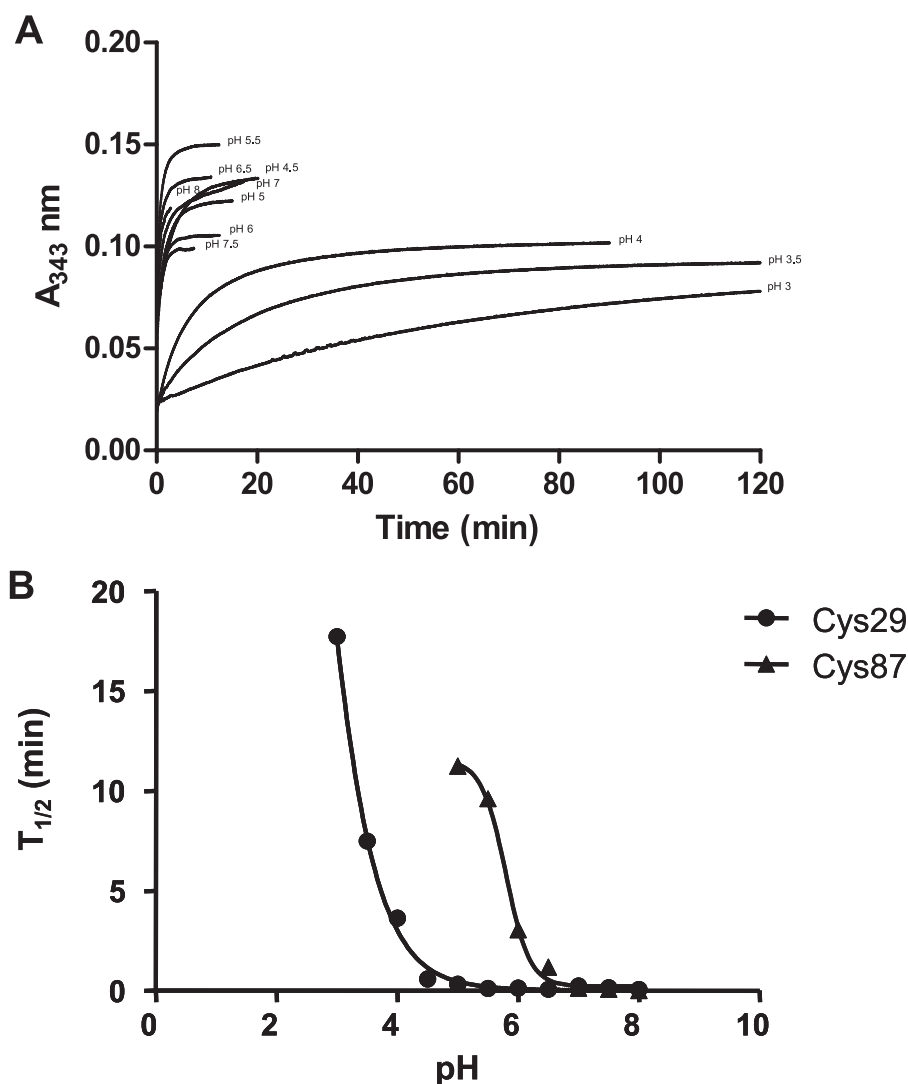
A

B

FIGURE 6. **pK_a determination of GrxS12 sulfhydryl groups.** *A*, reaction of GrxS12 C87S with PDT-bimane was monitored at 343 nm at pH values ranging from 3.0 to 8.0. The increase at 343 nm results from the release of pyridyl-2-thione from PDT-bimane. Each curve was fit to the Michaelis-Menten equation. *B*, $t_{1/2}$ for the reactions of PDT-bimane with GrxS12 C29S and C87S were plotted as a function of pH, and the results were fitted to a sigmoidal curve. From this plot, sulfhydryl pK_a values of 2.84 ± 0.08 and 5.63 ± 0.17 were determined for Cys[29] and Cys[87], respectively.

stabilized by conserved Tyr[31] and Glu[34] of the glutathionylated enzyme. This structural observation suggests that Cys[87] potentially possesses some reactivity. This is probably true, since in the classical Grx HED assay (see results above), residual activity is detected for the C29S variant. The distance between the Sγ atoms of both cysteine residues of the enzyme is ~8 Å, both cysteines being separated by the active site Tyr[31].

Comparison of the GSH Binding Site with Other Glutaredoxins—Of the available dithiol Grx structures, only those with a GSH present have been retrieved (see supplemental Fig. 2). In three cases, the second active site cysteine is mutated, and the GSH is covalently bound (human Grx1 (32), *E. coli* Grx1 (33), and *E. coli* Grx3 (34)); in one case, the GSH is not covalently bound to the wild type enzyme (human Grx2) (20). In these Grx structures, including the poplar GrxS12 structure, GSH is in an antiparallel orientation with respect to the main chains of the well preserved -TVP- loop segment for hydrogen bond formation (see supplemental Fig. 2). Favorable contacts with GSH are enhanced by the presence of a *cis*-Pro near the substrate binding site, the geometry of the latter residue increasing the stringency of the fold and ensuring the correct conformation of the preceding valine. The -GCT- segment is conserved with only some variations (Ser, Ala, or Asp) at the position of Thr. A polar residue present at the edge of a GSH binding groove coming into contact with Glu_{GSH} might be important to harbor the tripeptide molecule at the groove, by making hydrogen bonds with the amino group. This is indeed the case for all liganded Grx structures except for human Grx1. The position and orientation of the GSH diverge slightly at the glycine residue of GSH in all of the above mentioned liganded structures. The carboxylate group of Gly_{GSH} is interacting with the side chain of Arg[67] in human Grx1, whereas no similar interaction is found in other Grx complex structures.

Iron-Sulfur Cluster Assembly in GrxS12—The natural occurrence of an iron-sulfur cluster in poplar GrxC1 (YCGYC active site) and the possibility to incorporate such a prosthetic group in other Grxs from subgroup I when their active site is mutated from YC(P/F)YC into YCGYC but the absence of cluster in a WCGYS-mutated variant of GrxS12 raised the question of the role of the Trp residue and possibly of the cysteine to serine

cysteinyl and glutamyl moieties of GSH; see Table 4). Situated at the loop between β4 and α3, the backbone amino groups of Cys[87] and Thr[88] stabilize the glutamyl group of GSH through hydrogen bonds. These interactions are strengthened by another hydrogen bond between the side chain of Thr[88] and the N terminus of GSH (Table 4). The two residues immediately preceding Cys[87], [85]GG[86] (GG kink), are strictly conserved in all GrxS12 orthologs and in the majority of the subclass I Grx members. This GG kink is in proximity of the *cis*-Pro[75] (Fig. 7). *cis*-Pro[75] plays an important structural role (30, 31), and the GG kink may be important in determining the backbone geometry of the following residues that belong to the α-helix 3. On the other hand, no interaction was observed between the Gly_{GSH} and residues of GrxS12, thus suggesting that the GSH molecule is rather flexible on its C terminus side.

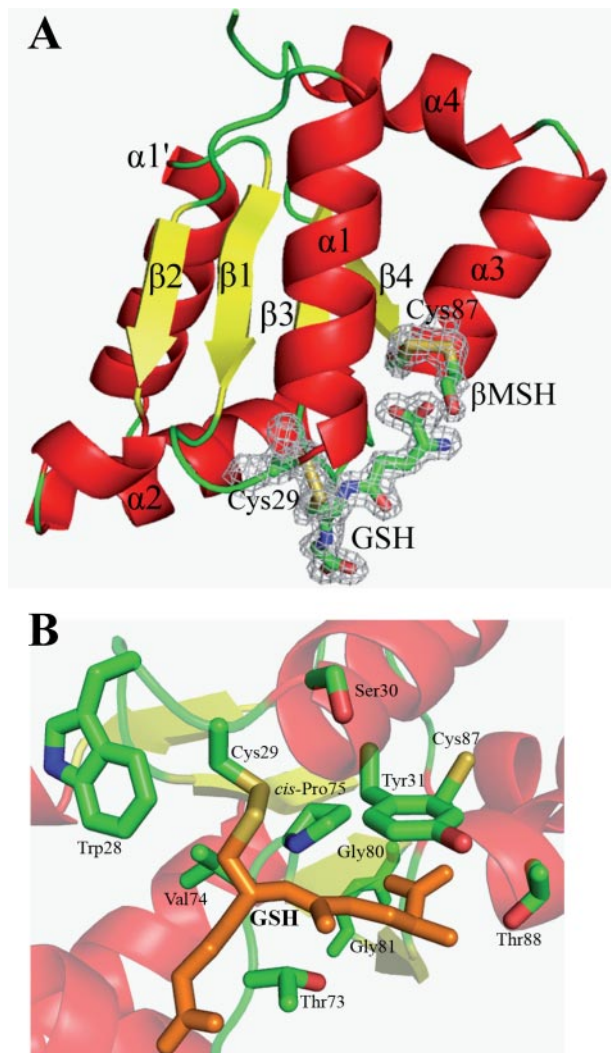In the model of GrxS12·GSH·βMSH, a βMSH molecule is covalently bound to the extra C terminus cysteine (Cys[87]) and

FIGURE 7. **Schematic representations of GrxS12·GSH·βMSH structure (A), highlighting the active site of the protein in B.** All α-helices are shown in *red*, whereas β-strands are in *yellow* and connecting loops are in *green*. Corresponding secondary structures are labeled. Both Cys[29] and Cys[87], GSH, and βMSH molecules are highlighted in *sticks*, with final $2F_o - F_c$ electron densities (1.2σ level) covering chosen residues and ligands for clarity. The catalytic Cys[29] and the bound GSH molecule are highlighted in *orange* in B for clarity.

TABLE 4

Hydrogen bonding interactions at the GrxS12-GSH interface

Interacted atoms		Distance	
GrxS12	GSH	GrxS12·GSH	GrxS12·GSH·βMSH
Cysteine residue		*Å*	
Val[74] N	O2	2.89	2.80
Val[74] O	N2	2.83	2.81
Glutamate residue			
Cys[87] N	O11	2.83	2.83
Cys[87] N	O12	3.21	3.21
Thr[88] N	O12	2.80	2.87
Thr[88] O$_{\gamma1}$	N1	3.09	3.44

substitution in the second position of GrxS12 active site (35). Although the latter residue is not involved in the cluster ligation, it is probably involved in its stabilization (35). To test this, two mutations have been introduced in GrxS12, leading to YCSYS and YCGYC active sites. The UV-visible spectra obtained at the end of an aerobic purification of the two proteins indicate that they possess the typical [2Fe-2S] cluster

observed previously in GrxC1 (supplemental Fig. 3) (data not shown). This supports the proposal that the active site Trp structurally prevents the incorporation of an iron-sulfur cluster in GrxS12. Moreover, when the monomer of the GrxS12 structure is superimposed onto the poplar GrxC1 structure, which contains an iron-sulfur cluster bridged between two monomers, it is obvious that the side chain of Trp[28] acts as the major deterrent that prevents the incorporation of the cluster in GrxS12 (Fig. 8).

DISCUSSION

With about 30 genes coding for Grxs, distributed in three major subclasses, higher plants have an expanded Grx family compared with other organisms that do not contain more than seven Grxs, as in *Saccharomyces cerevisiae* (36). When starting with such multigene families, one objective is to understand whether those genes and proteins have specific or redundant functions. The specificity is generally thought to be related to differences in activity, to differential gene and protein expression or protein localization (37). Some other explanations are linked to novel and unexpected functions. In poplar chloroplast, GrxS14 and GrxS16 are able to incorporate an iron-sulfur cluster and to transfer it to acceptor proteins (27). In addition, the apoproteins are not reduced by glutathione but rather by ferredoxin thioredoxin reductases (FTR).[6] Although belonging to subclass I Grxs, which contain dithiol Grxs, GrxS12 lacks the C terminus active site cysteine and displays a monothiol [28]WCSYS[32] motif. Nevertheless, there is an additional C terminus cysteine in position 87 (poplar GrxS12 numbering), present in all GrxS12 orthologs and conserved in many other dithiol or monothiol Grxs, including CGFS Grxs (subclass II). From a physiological point of view, it is worth mentioning that, in the chloroplast, GrxS12 is very different from the CGFS Grxs, since it efficiently reduces chloroplastic thiol-dependent antioxidant enzymes using glutathione as a substrate, indicating that plant GrxS12 may have several specific functions related to oxidative stress and signaling by regulating the thiol status of key proteins through deglutathionylation reactions.

Overall, the poplar GrxS12 structure shows no significant difference as compared with other known Grx structures. A glutathione is covalently bound to the active site cysteine of GrxS12. Structural analyses of numerous glutathione-liganded Grxs (20, 31, 32, 38, 39), including poplar GrxS12, reveal that their glutathione binding sites share the following characteristics: (i) the presence of a C*XX*(C/S) active site motif localized at the N terminus of helix α1'; (ii) the presence of a Tyr or a Phe at close vicinity of the catalytic Cys; (iii) the presence of [73]TVP[75] (numbering in GrxS12) loop motif with the Pro always in the *cis* conformation; (iv) the presence of a GG kink (in the loop between β3 and β4) at the proximity of the active site; and (v) conservation of charged residues at both edges of the substrate binding groove (GSH binding pocket).

Role of GrxS12 Active Site Organization for Regeneration Mechanism—The WCSYS active site sequence of GrxS12 is unique to plants and well conserved in all GrxS12 orthologs. The closest active sites are in mammalian Grx2 (SCSYC), in *S.*

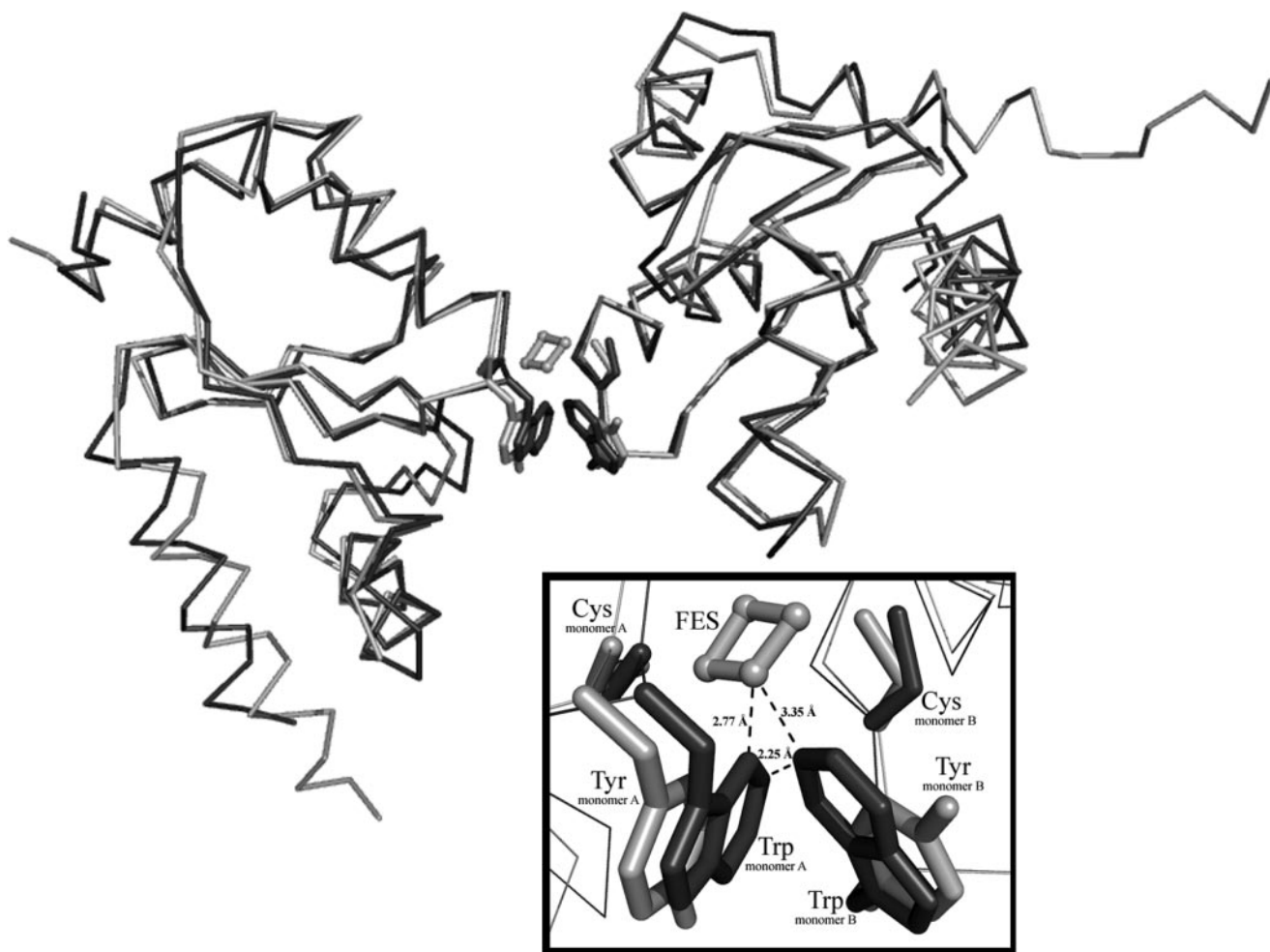[6] N. Rouhier, M. Zaffagnini, and S. D. Lemaire unpublished results.

FIGURE 8. **Superimposition of the hypothetical dimer of GrxS12 (*dark gray*) to the poplar GrxC1 dimer (*light gray*).** A *close-up view* detailing the ISC at the active site of poplar GrxC1 is presented in the *inset*. Upon the superimposition of the hypothetical dimer of GrxS12, Trp[28] of GrxS12 is the major hindrance of dimerization and the incorporation of the ISC. The dimer of poplar GrxC1 is bridged by a [2Fe-2S] cluster depicted as *spheres* with *sticks* (*light gray*) showing the coordination. The close distances between the ISC and both Trp residues of GrxS12 are labeled.

cerevisiae Grx6 (TCSYS), and in *Azorhizobium caulinodans* (WCSYC, accession number YP_001527212).

The position corresponding to Trp[28] in GrxS12 is usually occupied by Phe, Tyr, Ser, Thr, or even Gly in other known Grxs. In GrxS12, Trp[28] cooperates with Tyr[31] at the active site for the stabilization of the mixed disulfide between Cys[29] and Cys_{GSH}. This enables a favorable interaction between the hydrophobic and highly polarizable sulfurs and the hydrophobic and polarizable phenol ring of Tyr[31] and the indole ring of Trp[28], providing an additional determinant of peptide specificity toward GSH (particularly toward the γ-GluGSH moiety) or glutathionylated substrates. Interestingly, we were not able to obtain a GrxS12 crystal structure without a bound GSH molecule, and moreover a reduced GrxS12 is strongly precipitating over time, suggesting that the glutathionylated state might be more stable. By contrast, the W28Y mutant of GrxS12 is rather stable. It is also interesting to note that Trp (corresponding to the Trp[28] in GrxS12) has been attributed as a key residue in thioredoxins for the recognition of its substrate (40, 41). Therefore, one can envisage that Trp[28] could play a similar additional role in GrxS12.

The Ser[30] in GrxS12 replaces the classical Pro found in most traditional Grxs. Mutagenesis on human mitochondrial Grx2 demonstrated that this Pro to Ser replacement in the active site dipeptide is the major determinant for the affinity toward glutathionylated substrates (4). This difference, however, is rather small to trigger drastic modification in the three-dimensional structure of the GrxS12 active site, as shown for human Grx2 (20). Nevertheless, the serine residue in the active site motif could provide more flexibility to the main chain. All plant Grxs tested so far, including GrxS12, exhibit similar deglutathionylation activities with the classical *in vitro* substrate of Grx (HED), regardless of their active site motifs (CPYC, CSYS) (4, 7, 38).[7] For deglutathionylation of GAPDH, GrxS12 appeared slightly less efficient than classical Grxs harboring a CPYC active site, but its deglutathionylation activity is comparable with that reported for a chloroplastic CGFS containing Grx (7).

In fact, the regeneration mechanism proposed in previous studies for two identified partners of GrxS12, methionine sulfoxide reductase MsrB1 and peroxiredoxin Prx IIE, most likely

---

[7] N. Rouhier, unpublished data.

occurs via a glutathionylated protein intermediate (42, 43). This is supported by the capacity of GrxS12 but also of most other Grxs to catalyze efficiently deglutathionylation reactions.

Iron-Sulfur Cluster Assembly—Another important point is that human Grx2 (SCSYC active site), poplar GrxC1 (YCGYC), *S. cerevisiae* Grx6 (TCSYS), and *Trypanosoma brucei* Grx1 (MCAYS) are able to bind an iron-sulfur cluster, most likely a [2Fe-2S] cluster (20, 35, 44, 45). The crystal structures of Grx2 and GrxC1 in the holoform are similar and showed that the incorporation of the cluster requires the dimerization of the Grx and the presence of two external glutathione molecules (20, 35, 46). It has been demonstrated that all other poplar Grxs from subgroup I (GrxC2, -C3, and -C4; YCP(Y/F)C active sites), except GrxS12 (WCSYS), were also able to incorporate an iron-sulfur cluster when the active site was changed into CGYC, leading to the conclusion that the presence of a glycine or another small residue such as a serine but not a proline is critical for iron-sulfur cluster incorporation (35). It was also suggested in the same study that the presence of the tryptophan could prevent this incorporation. The mutation of the GrxS12 WSCYS active site into YCSYS or YCGYC, which allowed the assembly of an iron-sulfur center in these variants, confirmed this hypothesis. In addition, the resolution of the GrxS12 structure allowed us to model a hypothetic dimer in which the bulky tryptophan residue (Trp[28]) has been clearly identified as the major deterrent for the incorporation of the ISC in the active site of GrxS12 (Fig. 8). Moreover, bad contacts between the two indole side chains of Trp[28] of the two subunits also suggest that dimerization of GrxS12 is almost impossible without a conformational change of the Trp side chain (Fig. 8). Apart from the above-mentioned Trp, the presence of a *cis*-Pro in the C terminus of proteins of the Trx superfamily was proposed recently to prevent metal binding in these proteins, whereas almost all Grxs that incorporate an iron-sulfur cluster do possess it (47).

Is There a Role for the Additional Conserved Cysteine?—Many Trxs and Grxs have at least one additional conserved Cys residue outside the active site whose exact role has not always been elucidated. Some CGFS Grxs have been reported to possess a disulfide bridge involving an extra active site cysteine at the same position as in GrxS12 (5–7). For example, in *S. cerevisiae* Grx5, the importance of this disulfide is not clear, since it is required *in vitro* for deglutathionylation activity but not *in vivo* for the iron-sulfur biogenesis (48). For *C. reinhardtii* Grx3, it is also crucial *in vitro*, acting as a resolving cysteine for deglutathionylation reactions and then for its ferredoxin thioredoxin reductase-dependent regeneration (7). Many other Grxs from several organisms having additional cysteines have been found *in vitro* to undergo different types of oxidations and can be glutathionylated or nitrosylated or form intramolecular or intermolecular disulfide bridges (20, 30, 49–51).

The additional cysteine (Cys[87]) in GrxS12 (corresponding to the position of Cys[83] in *E. coli* Grx1) is solvent-exposed and is situated ~8.4 Å away from the catalytic Cys[29], separated by the aromatic side chain of Tyr[31]. The corresponding conserved active site Tyr residue has been reported to undergo conformational rearrangement in *E. coli* Grx3 from the free to the substrate-bound form or *vice versa* (52). Therefore, based on this Tyr flexibility, one could envisage that GrxS12 could undergo similar *in situ* redox-driven conformational changes. Nevertheless, the hypothesis that Cys[87] is able to reduce the Cys[29]-SSG mixed disulfide spontaneously is unlikely for the following reasons: (i) the C87S GrxS12 variant appeared as efficient as the WT protein in all activity assays; (ii) the recombinant protein is partially glutathionylated on the first active site cysteine, and once the protein is fully glutathionylated on Cys[29], the mixed disulfide is stable; (iii) we have been unable to form a fully oxidized form of GrxS12 (*i.e.* an intramolecular disulfide Cys[29]–Cys[87]), neither using a treatment with DTT_{ox} nor during crystallization. Nevertheless, because of its low pK_a (~5.6), Cys[87] of GrxS12 is fairly reactive. This is supported by the residual activity observed for GrxS12 C29S and by the presence of a βMSH covalently bound to Cys[87]. Therefore, the possibility cannot be excluded that this cysteine residue may have another role(s) apart from the GSH-specific oxidoreductase activity of GrxS12, serving as a target of post-translational modification (*e.g.* nitrosylation), as observed for human Grx1 and hence regulating Grx activity (50).

Conclusions—GrxS12 structures described in this study are the first structures of a plant monothiol Grx belonging to subclass I and the first crystallographic structure of a GSH-protein mixed disulfide in a natural C*XX*S active site motif. This study enabled the identification of a highly conserved GSH binding site in GrxS12 orthologs ([28]WCSY[31], [73]TVP[75], and [86]GCT[88]), similar to that described before. Concerning the active site residues, Trp[28] prevents the incorporation of an iron-sulfur cluster, and Tyr[31], although having a certain degree of flexibility, prevents the formation of an intramolecular disulfide between Cys[29] and Cys[87]. Nevertheless, we cannot completely rule out the possibility of Cys[87] playing a role as a recycling cysteine only under certain circumstances (*e.g.* substrate-dependent conditions (nonglutathionylated substrates)). Thus, contrary to another chloroplastic Grxs (*C. reinhardtii* Grx3 with a CGFS active site), which probably uses a dithiol mechanism for deglutathionylation reactions (an intramolecular disulfide bridge is reduced by ferredoxin thioredoxin reductase), it appears from the structure and the activity of the cysteinic variants that the GrxS12-dependent deglutathionylation occurs through a monothiol mechanism involving only the first active site cysteine. It would first attack the target protein-glutathione mixed disulfide, the Grx becoming itself glutathionylated before a glutathione molecule solves this mixed disulfide to regenerate the reduced Grx.

REFERENCES

1. Bushweller, J. H., Aslund, F., Wuthrich, K., and Holmgren, A. (1992) *Biochemistry* **31,** 9288–9293
2. Rouhier, N., Gelhaye, E., and Jacquot, J. P. (2002) *FEBS Lett.* **511,** 145–149
3. Lillig, C. H., Prior, A., Schwenn, J. D., Aslund, F., Ritz, D., Vlamis-Gardikas, A., and Holmgren, A. (1999) *J. Biol. Chem.* **74,** 7695–7698
4. Johansson, C., Lillig, C. H., and Holmgren, A. (2004) *J. Biol. Chem.* **279,** 7537–7543
5. Tamarit, J., Bellí, G., Cabiscol, E., Herrero, E., and Ros, J. (2003) *J. Biol.*

Chem. **278,** 25745–25751

6. Fernandes, A. P., Fladvad, M., Berndt, C., Andrésen, C., Lillig, C. H., Neubauer, P., Sunnerhagen, M., Holmgren, A., and Vlamis-Gardikas, A. (2005) *J. Biol. Chem.* **280,** 24544–24552

7. Zaffagnini, M., Michelet, L., Massot, V., Trost, P., and Lemaire, S. D. (2008) *J. Biol. Chem.* **283,** 8868–8876

8. Jung, C. H., and Thomas, J. A. (1996) *Arch. Biochem. Biophys.* **335,** 61–72

9. Martin, J. L. (1995) *Structure* **3,** 245–250

10. Rouhier, N., Gelhaye, E., and Jacquot, J.-P. (2004) *Cell. Mol. Life Sci.* **61,** 1266–1277

11. Rodríguez-Manzaneque, M. T., Ros, J., Cabiscol, E., Sorribas, A., and Herrero, E. (1999) *Mol. Cell. Biol.* **19,** 8180–8190

12. Lemaire, S. D. (2004) *Photosynth. Res.* **79,** 305–318

13. Rouhier, N., Couturier, J., and Jacquot, J.-P. (2006) *J. Exp. Bot.* **57,** 1685–1696

14. Schenk, P. M., Baumann, S., Mattes, R., and Steinbiss, H. H. (1995) *BioTechniques* **19,** 196–200

15. Augusto, L., Decottignies, P., Synguelakis, M., Nicaise, M., Le Maréchal, P., and Chaby, R. (2003) *Biochemistry* **42,** 3929–3938

16. Mansoor, S. E., and Farrens, D. L. (2004) *Biochemistry* **43,** 9426–9438

17. Otwinowski, Z., and Minor, W. (1997) *Methods Enzymol.* **276,** 307–326

18. Collaborative Computational Project 4 (1994) *Acta Crystallogr. Sect. D* **50,** 760–763

19. Vagin, A., and Teplyakov, A. (1997) *J. Appl. Crystallogr.* **30,** 1022–1025

20. Johansson, C., Kavanagh, K. L., Gileadi, O., and Opperman, U. (2007) *J. Biol. Chem.* **282,** 3077–3082

21. Perrakis, A., Morris, R., and Lamzin, V. S. (1999) *Nat. Struct. Biol.* **6,** 458–463

22. Murshudov, G. N., Vagin, A. A., and Dodson, E. J. (1997) *Acta Crystallogr. Sect. D* **53,** 240–255

23. Emsley, P., and Cowtan, K. (2004) *Acta Crystallogr. Sect. D* **60,** 2126–2132

24. Laskowski, R. A., MacArthur, M. W., Moss, D. S., and Thornton, J. M. (1993) *J. Appl. Crystallogr.* **26,** 283–291

25. Delano, W. L. (2002) *PyMol*, DeLano Scientific, Palo Alto, CA

26. Kleywegt, G. J., and Jones, T. A. (1997) *Acta Crystallogr. Sect. D* **53,** 179–185

27. Bandyopadhyay, S., Gama, F., Molina-Navarro, M. M., Gualberto, J. M., Claxton, R., Naik, S. G., Huynh, B. H., Herrero, E., Jacquot, J. P., Johnson, M. K., and Rouhier, N. (2008) *EMBO J.* **27,** 1122–1133

28. Zaffagnini, M., Michelet, L., Marchand, C., Sparla, F., Decottignies, P., Le Marechal, P., Miginiac-Maslow, M., Noctor, G., Trost, P., and Lemaire, S. D. (2007) *FEBS J.* **274,** 212–226

29. Srinivasan, U., Mieyal, P. A., and Mieyal, J. J. (1997) *Biochemistry* **36,** 3199–3206

30. Bushweller, J. H., Billeter, M., Holmgren, A., and Wüthrich, K. (1994) *J. Mol. Biol.* **235,** 1585–1597

31. Nordstrand, K., Aslund, F., Holmgren, A., Otting, G., and Berndt, K. D. (1999) *J. Mol. Biol.* **286,** 541–552

32. Yang, Y., Jao, S., Nanduri, S., Starke, D. W., Mieyal, J. J., and Qin, J. (1998) *Biochemistry* **37,** 17145–17156

33. Sodano, P., Xia, T. H., Bushweller, J. H., Bjornberg, O., Holmgren, A., Billeter, M., and Wuthrich, K. (1991) *J. Mol. Biol.* **221,** 1311–1324

34. Aslund, F., Nordstrand, K., Berndt, K. D., Nikkola, M., Bergman, T., Ponstingl, H., Jornvall, H., Otting, G., and Holmgren, A. (1996) *J. Biol. Chem.* **271,** 6736–6745

35. Rouhier, N., Unno, H., Bandyopadhyay, S., Masip, L., Kim, S. K., Hirasawa, M., Gualberto, J., Lattard, V., Kusunoki, M., Knaff, D. B., Georgiou, G., Hase, T., Johnson, M. K., and Jacquot, J. P. (2007) *Proc. Natl. Acad. Sci. U. S. A.* **104,** 7379–7384

36. Morel, M., Kohler, A., Martin, F., Gelhaye, E., and Rouhier, N. (2008) *New Phytol.* **180,** 391–407

37. Rouhier, N., Lemaire, S. D., and Jacquot, J. P. (2008) *Annu. Rev. Plant. Biol.* **59,** 143–166

38. Nikkola, M., Gleason, F. K., Saarinen, M., Joelson, T., Bjornberg, O., and Eklund, H. (1991) *J. Biol. Chem.* **266,** 16105–16112

39. Xia, T. H., Bushweller, J. H., Sodano, P., Billeter, M., Bjornberg, O., Holmgren, A., and Wuthrich, K. (1992) *Protein Sci.* **1,** 310–321

40. Krause, G., and Holmgren, A. (1991) *J. Biol. Chem.* **266,** 4056–4066

41. Menchise, V., Corbier, C., Didierjean, C., Jacquot, J. P., Benedetti, E., Saviano, M., and Aubry, A. (2000) *Biopolymers* **56,** 1–7

42. Vieira Dos Santos, C., Laugier, E., Tarrago, L., Massot, V., Issakidis-Bourguet, E., Rouhier, N., and Rey, P. (2007) *FEBS Lett.* **581,** 4371–4376

43. Gama, F., Bréhélin, C., Gelhaye, E., Meyer, Y., Jacquot, J. P., Rey, P., and Rouhier, N. (2008) *Physiol. Plant.* **133,** 599–610

44. Mesecke, N., Mittler, S., Eckers, E., Herrmann, J. M., and Deponte, M. (2008) *Biochemistry* **47,** 1452–1463

45. Comini, M. A., Rettig, J., Dirdjaja, N., Hanschmann, E. M., Berndt, C., and Krauth-Siegel, R. L. (2008) *J. Biol. Chem.* **283,** 27785–27798

46. Feng, Y., Shong, N., Rouhier, N., Hase, T., Kusunoki, M., Jacquot, J. P., Jin, C., and Xia, B. (2006) *Biochemistry* **45,** 7998–8008

47. Su, D., Berndt, C., Fomenko, D. E., Holmgren, A., and Gladyshev, V. N. (2007) *Biochemistry* **46,** 6903–6910

48. Bellí, G., Polaina, J., Tamarit, J., De La Torre, M. A., Rodríguez-Manzaneque, M. T., Ros, J., and Herrero, E. (2002) *J. Biol. Chem.* **277,** 37590–37596

49. Sun, C., Berardi, M. J., and Bushweller, J. H. (1998) *J. Mol. Biol.* **280,** 687–687

50. Hashemy, S. I., Johansson, C., Berndt, C., Lillig, C. H., and Holmgren, A. (2007) *J. Biol. Chem.* **282,** 14428–14436

51. Melchers, J., Dirdjaja, N., Ruppert, T., and Krauth-Siegel, R. L. (2007) *J. Biol. Chem.* **282,** 8678–8694

52. Nordstrand, K., Sandström, A., Åslund, F., Holmgren, A., Otting, G., and Berndt, K. D. (2000) *J. Mol. Biol.* **303,** 423–432